

RULE-BASED IDENTIFICATION OF BEARING FAULTS USING CENTRAL TENDENCY OF TIME DOMAIN FEATURES

Muhammad Masood Tahir¹, Ayyaz Hussain², Saeed Badshah³, Qaisar Javaid²

ABSTRACT

Vibration-based time domain features (TDFs) are commonly used to recognize patterns of machinery faults. This study exploits central tendency (CT) of TDFs to develop a Rule-based Diagnostic Scheme (RDS), which identifies localized faults in ball bearing. The RDS offers an accurate and efficient diagnostic procedure, and purges the requirement of expensive training of conventional classifier. A test rig is used to acquire vibration data from bearings having localized faults, and various TDFs are extracted. It is worth mentioning that fluctuations in random vibration signals may alter the feature values. Therefore, each of the TDFs is processed statistically to approximate its reliable central values (CVs) against the respective faults. In this way, every feature provides a set of CVs, which are equal in number to that of faults. Separating distances among normalized CVs (NCVs) in a set provide the criteria to select or discard that particular feature before further processing. The selected sets of NCVs are finally used as references to generate rule-set for testing the unknown vibration samples. The results are evident that the proposed RDS may be an effective alternative to the existing classifier-based fault diagnosis, even if the vibration signals are contaminated with considerable background noise.

Key Words: *Rule-based diagnostics, Feature processing, Fault diagnosis, Central tendency.*

INTRODUCTION

Ball bearing is a vital part of rotating machinery. Unexpected failure of bearing can lead to catastrophic and financial losses. Therefore, precise and early identification of bearing's faults has been the area of research over the years¹. Vibration analysis technology has been used widely for machine condition of machinery². Difficulty is that these faults produce very weak impulses in vibration signals that is very hard to detect. This makes application of traditional frequency analysis methods somewhat limited for the purpose¹. To enhance the detection process, many methods have been introduced regarding the pre-processing of raw vibration data. Removal of signal noises, filtration of appropriate bands and wavelet decomposition are the popular pre-processing methods³⁻⁹. Additionally, signal processing techniques include spectral kurtosis¹⁰ analysis and cepstrum analysis¹¹. However, these techniques are useful only in case of well-developed mechanical faults¹². Pattern recognition (PR) methods¹³ are also utilized extensively to automate the faults detection process. But, presence of noise in machine learning system can also misleads classifiers during their training¹⁴⁻¹⁵. Numerous PR methods have been introduced so far which utilized vibration-based TDFs¹⁶⁻²⁵. Unfortunately, achieving an optimum fault

classification accuracy has been a challenge using a minimal set of features.

Statistical values of TDFs can be fluctuated because of randomness in vibration signals or noise. The proposed RDS exploits the CT of TDFs to develop a rule-based decision mechanism, which has not been reported so far to the best of our knowledge. A test rig is used to acquire vibration data for the localized faults of ball bearings. Each vibration signal is segmented into suitable numbers. Most commonly used TDF are then extracted from the segments of every signal to obtain feature distributions for respective faults. The TDFs include root mean square (RMS), variance, mean, skewness, median, kurtosis, range, crest factor, shape factor and impulse factor. The feature distributions are processed separately to calculate their CTs or CVs. Thus, each feature provides a set of CVs equal in number to the introduced faults. Separating distances among NCVs in every set are exploited then to select salient features. The selected sets, i.e. sets of NCVs, are employed finally to define threshold limits to form a rule-set for data testing. Contributions of this research is summarized as;

- The CT of TDF is exploited to develop a new RDS.

¹ Department of Electrical Engineering, International Islamic University Islamabad (IIUI).

² Department of Computer Science, IIUI.

³ Department of Mechanical Engineering, IIUI.

- The RDS is accurate and immune to background noise
- The RDS provides an efficient alternative solution to the classifier-based diagnostics.

The manuscript is organized as follows. The proposed method is explained along with relevant material in Section 2. The results are discussed in Section 3 along with the research findings, and at the end Section 4 draws the conclusions of the present study.

2. MATERIAL AND METHODS

The proposed RDS works in four steps, elaborated via Figure 1. Firstly, the vibration data were acquired from a set of bearings having localized faults. The feature processing was employed at second step, which works in three further stages. At third step, most significant features were chosen for generating efficient diagnostic rules. Finally, decision making was performed using the rule-set. The following subsections follow the details.

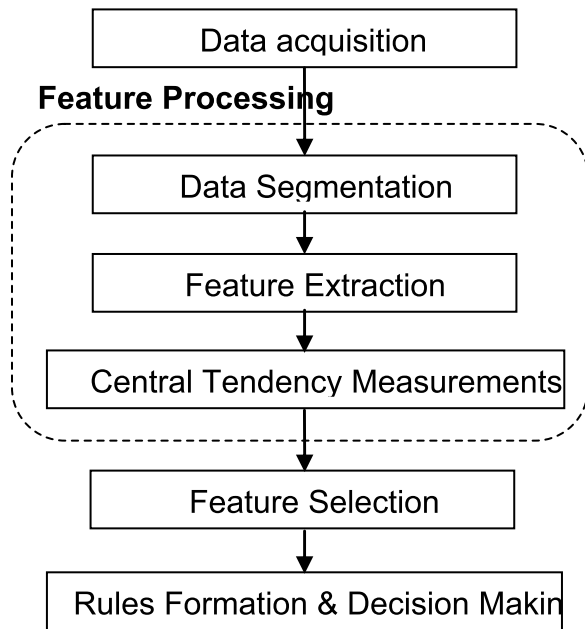


Figure 1. Main steps involved in RDS

2.1. Data Acquisition

A test rig was used to have vibration data from ball bearings containing localized faults. The faults included; fault at inner race (IRF), at outer race (ORF), at ball

(BLF) and mixture of these faults (MXF). The motor speed was 1000 rpm. Healthy shaft was loaded with 5kg weight placed in the center, as shown in schematic in Figure 2. Vibration data was acquired from the top of out-board bearing via stud-mounted piezoelectric acceleration sensor having sensitivity 100 For each fault, data sample of 10 seconds was acquired at the rate of 60 K Samples/sec.

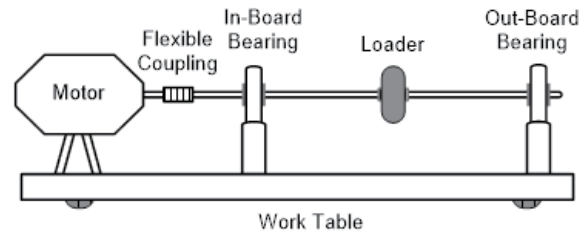


Figure 2. Schematic of experimental setup

The data was validated before further analysis, using conventional benchmark method known as envelope analysis¹. During the application of enveloping, fast kurtogram method²⁶ was applied to calculate the required frequency bands. The offensive fault frequencies are appeared in the enveloped spectra of vibration signals. The fault frequencies are known as fundamental train or cage frequency (FTF), ball-pass frequency on the inner-race (BPFIR), ball-pass frequency on the outer race (BPFOR) and ball-spinning frequency between the races (BSF). Table 1 shows the calculated fault frequencies using formulas below.

$$FTF = \frac{freq}{2} \left(1 - \frac{d}{P_d} \cos \gamma\right) \quad (1)$$

$$BPFIR = \frac{N_b \times freq}{2} \left(1 + \frac{d}{P_d} \cos \gamma\right) \quad (2)$$

$$BPFOR = \frac{N_b \times freq}{2} \left(1 - \frac{d}{P_d} \cos \gamma\right) \quad (3)$$

$$BSF = \frac{N_b \times freq}{2} \left(1 - \left(\frac{d}{P_d}\right)^2 \cos^2 \gamma\right) \quad (4)$$

where freq is rotating speed of motor or shaft, N_b is number of balls present in the bearing, d is diameter of ball, P_d is diameter of pitch and is γ ball's contact angle.

Table 1. Fault frequencies in ball bearing

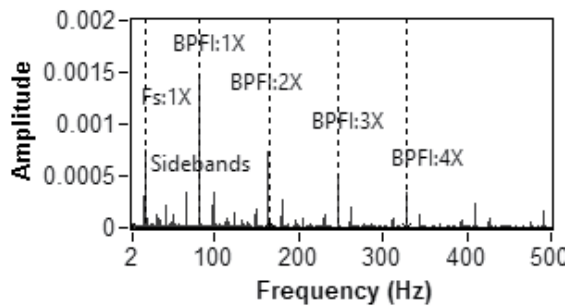
freq	FTF	BPFIR	BPFOR	BSF
16.7	6.4	82.5	50.9	33.2

Figure 3 show spectra of faulty bearings. Figure 3(a) indicates spectrum of the IRF. Several harmonics of BPFIR are there in conjunction with side-bands of the speed of shaft. Figure 3(b) shows spectrum of the ORF, showing some harmonics of BPFOR. The BLF is evident in spectrum in Figure 3(c), where twice the BSF has come into view with FTF side-bands. Figure 3(d) indicates the MXF fault, as ORF and BLF are dominant in the spectrum. Hence, acquired data contains every essential information regarding the bearing faults used in the study.

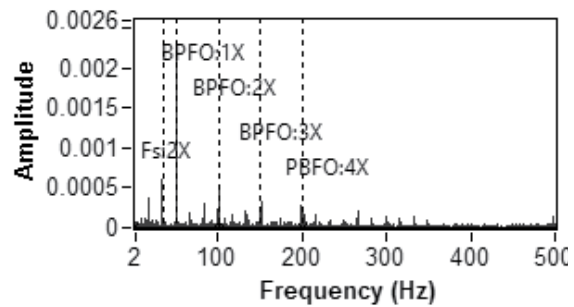
Features Processing

The CT-based features processing was the key step to generate the rule-set. The processing mechanism runs in three stages to process each TDF distribution separately. Schematic in the Figure 4 elaborates the processing of any single feature in three stages. Each of the stage has been explained in the following subsections.

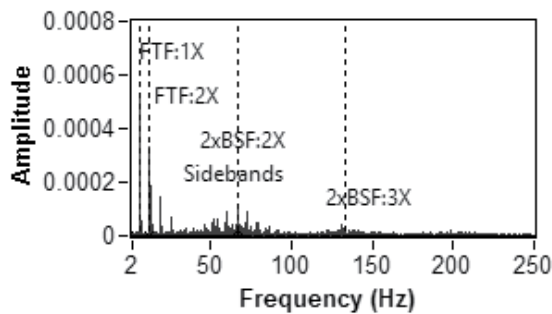
2.2.1. Data Segmentation



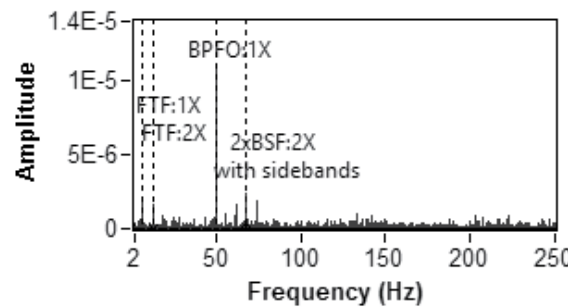
a) Enveloped frequency spectrum of IRF



b) Enveloped frequency spectrum of ORF



c) Enveloped frequency spectrum of BRF



d) Enveloped frequency spectrum of MXF

Figure 3. Enveloped frequency spectra of faulty bearings

Firstly, every vibration signal was segmented into N segments (N=40 in this study). As mentioned already that the data was sampled at 60 K Samples/sec, while motor speed was 1000 rpm. In this way, each of the segment contained vibration record of more than four revolutions of the shaft and contains 15000 observations, for reliable statistical computation of TDFs.

2.2.2. Feature Extraction

Ten TDFs were extracted from each segment of every vibration sample. TDFs features are sensitive to impulsive

oscillations in vibration signals, and frequently used for machinery fault diagnosis²⁷. Mathematically description of the extracted features is below.

$$1. \quad \text{RMS} = \left(\frac{1}{M} \sum_{p=1}^M [G(p)]^2 \right)^{\frac{1}{2}} \quad (5)$$

$$2. \quad \text{Mean } (\mu) = \frac{1}{M} \sum_{p=1}^M G(p) \quad (6)$$

$$3. \quad \text{Variance } (\sigma^2) = \frac{1}{M} \sum_{p=1}^M (G(p) - \mu)^2 \quad (7)$$

$$4. \quad \text{Skewness} = \frac{1}{M} \sum_{p=1}^M \left(\frac{G(p) - \mu}{\sigma} \right)^3 \quad (8)$$

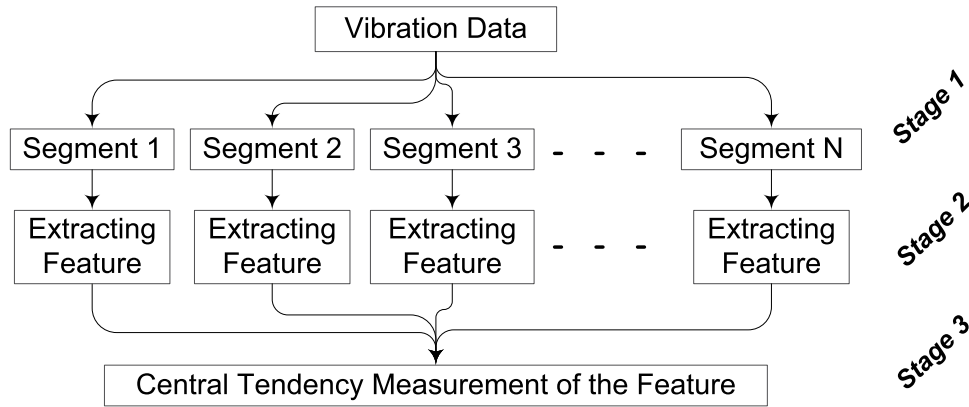


Figure 4. Single feature processing mechanism

5. Kurtosis = (9)

6. Crest Factor = $\frac{Max(|G|)}{RMS}$ (10)

7. Impulse Factor = $\frac{Max(|G|)}{\frac{1}{M} \sum_{p=1}^M |G(p)|}$ (11)

8. Shape Factor = $\frac{RMS}{\frac{1}{M} \sum_{p=1}^M |G(p)|}$ (12)

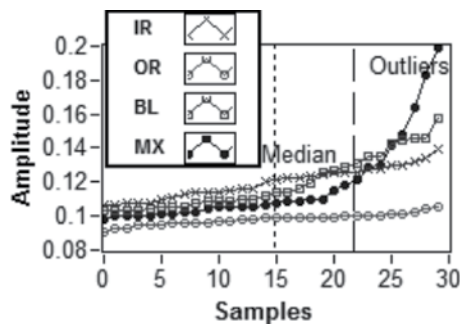
9. Median = $Magnitude\left(\frac{M+1}{2}\right)$ (13)

10. Range = $Maximum(G) - Minimum(G)$ (14)

where G is sequence of digital samples obtained for any vibration signal, $G(p)$ is the amplitude of p^{th} sample and M represents total number in samples a sequence contained.

Central Tendency Measurements

The CT of any data distribution portray the distribution



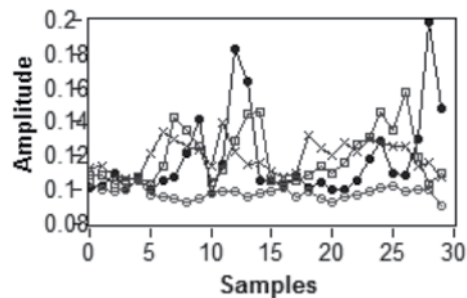
a) Ascending ordered elements of kurtosis

with a single value, which is represented mainly by mean, median or mode. Each of these measure can be more suitable as per application. For example, mean is useful when applied on symmetric data distribution. However, it is very sensitive to abnormal data or outlying values. Median, on the other hand, shows stability against the outliers²⁸.

Fluctuations occurred in random vibration signals may consequently produce feature outliers. The Figure 5(b) shows random elements of kurtosis features, extracted from every segment of all the faulty signals. Whereas, Figure 5(a) shows the median scores of the feature that are stable and almost insensitive to the outliers. Therefore, this research considered the respective median scores as CVs of the TDFs.

2.3. Feature Selection

Significant features were selected for reliable



b) Unsorted random elements of kurtosis

Figure 5. Kurtosis feature extracted from all the fault signals.

generation of fault identification rules. As the number of values present in a set of CVs were 4, i.e. equal in number to that of fault classes. Therefore, for convenient separation of the four faults, each set was normalized from 0 to 3 using the relation below.

$$Normalized_Value = 3 \times \left(\frac{Value \times Min(CV\ Set)}{Max(CV\ Set) - Min(CV\ Set)} \right) \quad (15)$$

Separation among the NCVs within any set was used to develop feature selection procedure. A feature having the ability to well separate the NCVs in its corresponding set was considered valuable for the diagnostic purpose. The algorithm elaborated the procedure via flow chart in Figure 6.

First of all, values in each set was sorted in ascending order to calculate relative distances between every pair.

A pair represents any two adjacent NCVs in a set. In this way, there exists three pairs in a NCV-set. Because the normalization of four NCVs is from 0 to 3 in a set. Therefore, an ideal distance between each pair was 1. Increasing distance in any pair above 1 will reduce distances between the neighboring pairs. Figure 7 shows separating distances among NCVs of the respective sets produced by every feature. Horizontal axis of the figure indicates the features by numbers assigned in Section 2.2.2. To select a particular feature, a minimum distance limit between all the pairs is required to be fulfilled in the respective set of NCVs to which that feature belonged. For the purpose, a user defined parameter named as *setDist* was defined to put a limit from 0 to 1. In case the distances between all pairs were larger than the defined limit, then that respective feature was chosen (if FS = True). For instance, setting value of *setDist* parameter to

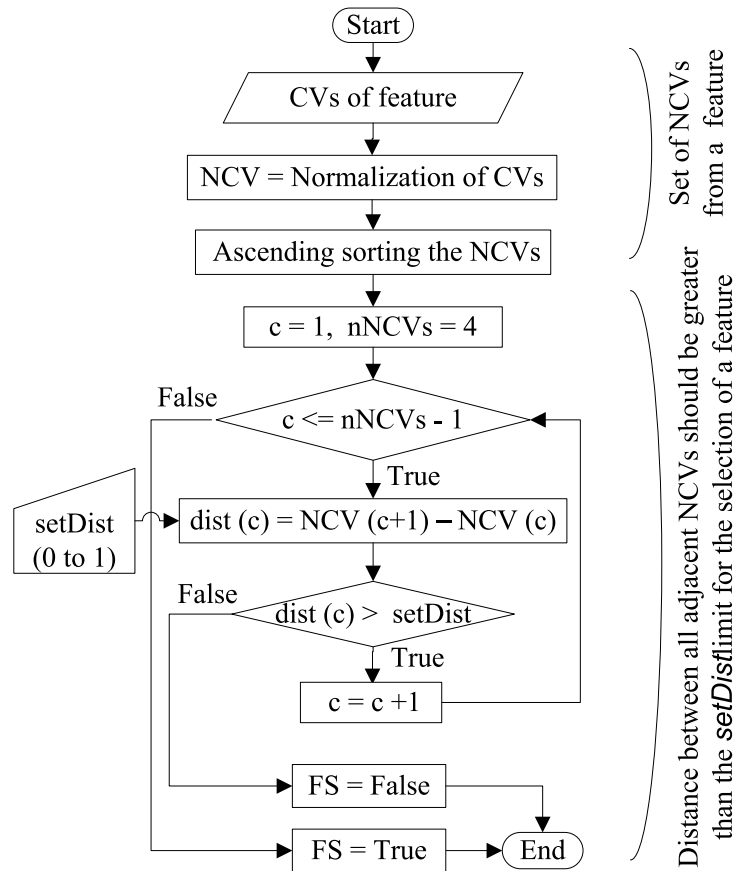


Figure 6. Flow chart of feature evaluation procedure

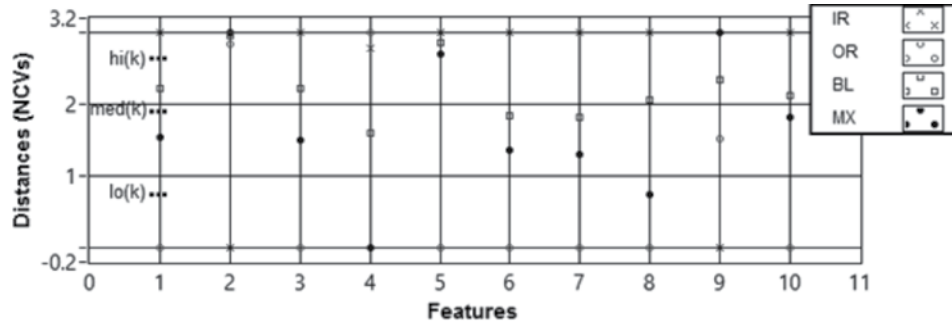


Figure 7. Normalized relative distances among the sets of NCVs of every feature

0.66, the feature evaluation algorithm returned three top ranking features that included RMS, variance and shape factor respectively (numbered as 1,3 and 8 in Figure 7 respectively). Though, several features demonstrated reasonably good separation among their respective NCV-sets, as shown by minimum distances in Table 2. The features include RMS, median, variance, shape factor, crest factor and impulse factor. When the *setDist* limit

approaches to its utmost value 1, then the criterion

Table 2. Minimum distances between any pair in a set of NCVs

Feature No.	Distance (0 to 1)	Status
1. RMS	0.6731	Selected
2. Mean	0.0452	Discarded
3. Variance	0.7177	Selected
4. Skewness	0.2268	Discarded
5. Kurtosis	0.1402	Discarded
6. Crest Factor	0.4843	Discarded
7. Impulse Factor	0.5167	Discarded
8. Shape Factor	0.7444	Selected
9. Median	0.6568	Discarded
10. Range	0.3146	Discarded

of feature selection turn out to be more strict for that feature to be selected and vice versa.

2.4. Rules Formation and Decision Making

The corresponding NCV-sets chosen against the three salient features were used to construct rules to identify bearing faults. Three most important features were RMS, variance and shape factor respectively. As there were three pairs in a NCV-set, which contains four values.

Thus, three reference limits (*ref_NCVs*) were obtained by averaging the NCVs of each pair, as shown graphically for RMS feature in Figure 7. The reference limits *lo(k)*, *med(k)* and *hi(k)* were obtained for every feature; *k=1* for RMS feature. Rule formation procedure utilized these references for decision making, as illustrated in Algorithm 1. The algorithm generated only four rules for the purpose, i.e. single rule for the identification of single fault.

To test the unknown vibration sample, three selected TDFs were extracted also from the test sample, i.e. RMS, variance and shape factor. The features were also processed through the feature processing step explained in Section 2.2. This produced three test CVs against these three features. Again, every test CV was normalized using Equation 16, i.e. between 0 and 3. During the process, the same corresponding values of *min* and *max* were used in the calculations that were obtained using the reference CV-sets. Finally, each of the normalized test CV (*test_NCV*) was compared with the corresponding reference set (*ref_NCVs*) to recognize the fault class to which that particular vibration sample might belonged. For example, the test NCV of RMS feature were compared with *ref_NCVs*, which were obtained using the RMS feature extracted from reference vibration data-set.

3. RESULTS AND DISCUSSION

The CT exhibited by TDFs was utilized to generate rules to classify localized fault in ball bearing. The vibration data was acquired using test rig for every fault.

The data was divided into segments, and the TDFs were extracted from every segment. This forms feature distributions, which may contain outlying values due

Algorithm 1 Rule-set formation with chosen features Inputs:

nFeatures=3

nNCVs=4

ref_NCV [3,4] (3 chosen sets of NCVs, each one contains 4 references)

test_NCV[3] (Set of 3 test NCVs obtained from 3 chosen features)

Output: Fault_type

for k=1→nFeatures do

for m=1→nNCVs-1 do

(limit(m) = (ref_NCVs(k,m)+ref_NCVs(k,m+1))/2

end for

lo(k) = limit(1)

med(k) = limit(2)

hi(k) = limit(3)

end for

if test_NCV(1) > hi(1) and test_NCV(2) < lo(2) and test_NCV(3) >hi(3) then Fault_type = IRF

else if test_NCV(1) < lo(1) and test_NCV(2) > hi(2) and test_NCV(3) < lo(3) then Fault_type = ORF

else if test_NCV(1) > med(1) and test_NCV(1) < hi(1) and test_NCV(2) > med(2) and test_NCV(2) < hi(2) and test_NCV(3) > med(3) and test_NCV(3) < hi(3)

then Fault_type = BLF

else if test_NCV(1) > lo(1) and test_NCV(1) < med(1) and test_NCV(2) > lo(2) and test_NCV(2) < med(2) and test_NCV(3) > lo(3) and test_NCV(3) < med(3)

then Fault_type = MXF

else Fault_type = Unknown

end if

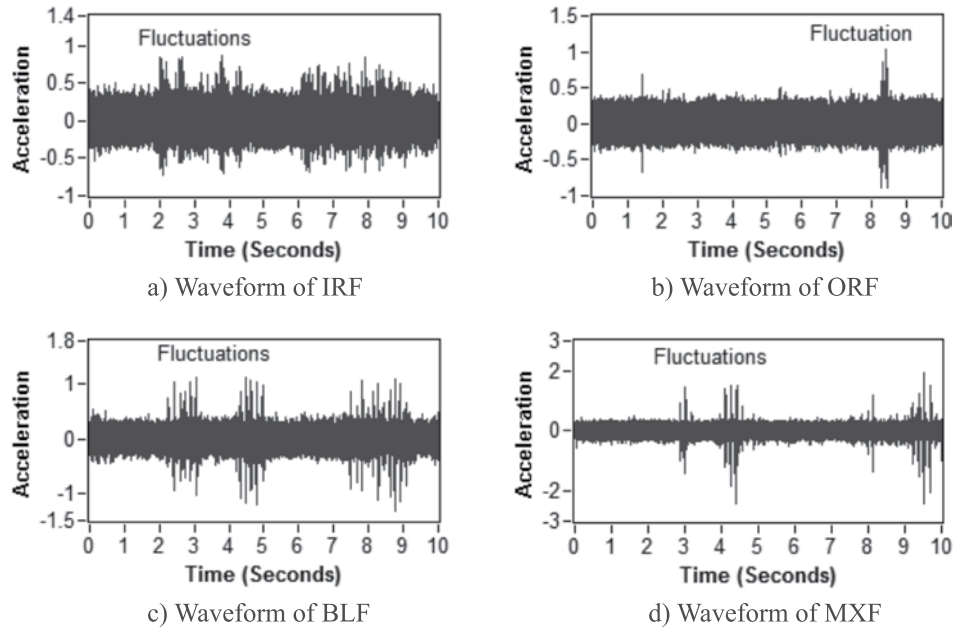


Figure 8. Waveforms of bearing faults

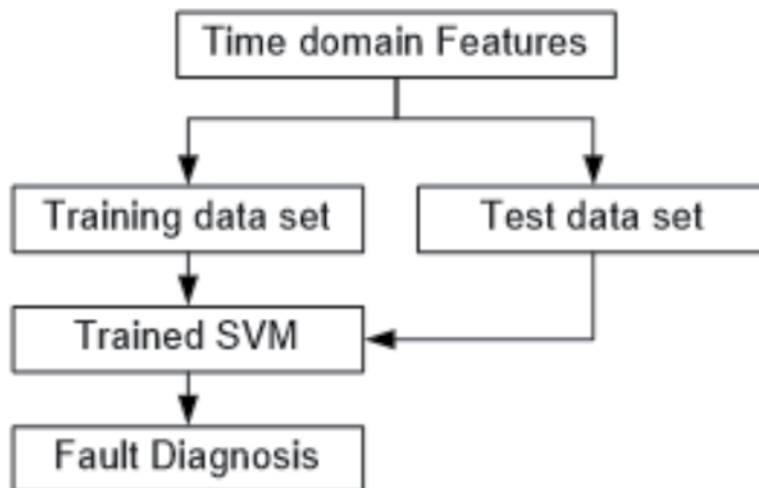


Figure 9. SVM multiclass classification model

to fluctuations present in random vibration signals, as shown in Figure 8. It was observed that median scores were almost insensitive to these feature outliers, as shown in Figure 5. Therefore, the median scores were characterized as steady CVs of the TDFs against the respective faults. These CVs were acted as references to produce rules to judge the type of fault. Notably, only the selected features participated in the diagnostic process for reliable and efficient results.

To evaluate the performance of RDS, total 160 test

samples were acquired, i.e. 40 vibration samples for each bearing fault. Each of the test sample was processed through feature processing step to create single set containing three *test_NCVs* against the three selected features. In this way, the Algorithm 1 utilized 3×160 *test_NCVs* in total. The algorithm provides 95.6% fault identification accuracy. Only three samples of BLF and four of MXF were remained unknown out of 160 samples.

To compare the performance of RDS, a supervised learning model support vector machine (SVM) was

Table 3. Vibration data samples used for RDS, and for SVM model

Vibration Samples	IRF	ORF	BLF	MXF
RDS References	1	1	1	1
RDS Testing	40	40	40	40
SVM Train & test	40	40	40	40

Table 4. Effect of Gaussian white noise of different levels on the RDS and SVM faults classification accuracy (%)

Features	40 (dB)	30 (dB)	20 (dB)	10 (dB)	05 (dB)
SVM	76.3	75.6	75.0	73.6	70.2
RDS	95.6	95.6	95.6	94.4	94.4

Ref	Method	Accuracy	Features	Classes
[29]	ANN	88.2-97.9	6	4
[8]	Wavelet analysis	56.1-99.9	5	3
[17]	ANN & SVM	98.6-100	66	2
[16]	ANN, GA & SVM	88.9-95.1	9-45	2
[19]	ANN	62-100	4	2
[20]	ANN	100	8	4
[21]	GA	97.4-100	18	2
[7]	Wavelets & HMM	46.5-99.5	5	4
[18]	SVM	98.9-100	25-156	2
[9]	SVM & wavelet denoising	100	2	7
[22]	Fuzzy & Decision tree	97.2	3	4
[23]	SVM & ANN	71.2-73.9	6	5
[24]	SVM & PSVM	89.1-100	7	3
[25]	SVM & Decision Tree	93.9-99.8	5	12
This study	The RDS	95.6	3	4

implemented using Weka software. Training data was prepared using the same vibration data, which were used to obtain reference NCVs. Similarly, test data was prepared from the same vibration data that was used to test the proposed RDS. The TDFs were transformed into instances by adding the respective fault class labels. In this way, 160 instances, 40 instances for each fault class, were fed to the classifier. The multiclass SVM produced 74.4% fault classification accuracy applying 10-fold cross-validation method for the training and testing purpose. Table 3 summarizes the vibration data samples involved in the RDS development, in its evaluation process, and in the SVM model.

Gaussian white noise was added at various signal to noise ratios (SNRs) in the vibration signals to show the robustness of the proposed method against the strong

background noise. Comparative accuracies using SVM and RDS is shown in Table 4. The results are evident that our proposed RDS is considerably immune to the added background noise.

Finally, results from similar sought of existing diagnostic schemes are compared with that of RDS. Table 5 elaborates the results in terms of classification accuracy against specific number of bearing faults and number of features involved. The proposed RDS provides excellent results and identified the four faults with 95.6% accuracy using only three features.

4. CONCLUSIONS

The CT of TDFs was investigated, and exploited to develop a new RDS to identify localized faults often

occur in ball bearing. Vibration data was captured for four faults using a test rig. The data was segmented, and various TDFs were extracted from these segments. The feature distributions were then separately processed statistically to obtain their CVs against the respective faults. Distances between NCVs in respective sets were utilized to build a feature selection mechanism, and to generate simple rule-set for the fault identification. The RDS produced excellent results even if the vibration signals were affected by strong background noises. The proposed methodology may eliminate the requirement of computationally complex training of classifier, and offers an efficient alternative to the existing PR-based fault diagnosis.

REFERENCES

1. Randall, R. B., 2011. "Vibration-based condition monitoring: industrial, aerospace and automotive applications". Wiley.
2. Wovk, V., 1991. "Machinery Vibration: Measurement and Analysis". McGraw-Hill Education.
3. Sawalhi, N., Randall, R. and Endo, H., 2007. "The enhancement of fault detection and diagnosis in rolling element bearings using minimum entropy deconvolution combined with spectral kurtosis". *Mechanical Systems and Signal Processing* 21: 2616-2633.
4. Wang, W. and Lee, H., 2013. "An energy kurtosis demodulation technique for signal denoising and bearing fault detection". *Measurement Science and Technology* 24: 025601.
5. Lou, X. and Loparo, K. A., 2004. "Bearing fault diagnosis based on wavelet transform and fuzzy inference". *Mechanical Systems and Signal Processing* 18: 1077-1095.
6. Smith, C., Akujuobi, C. M., Hamory, P. and Kloesel, K., 2007. "An approach to vibration analysis using wavelets in an application of aircraft health monitoring". *Mechanical Systems and Signal Processing* 21: 1255-1272.
7. Purushotham, V., Narayanan, S. and Prasad, S. A., 2005. "Multi-fault diagnosis of rolling bearing elements using wavelet analysis and hidden markov model based fault recognition". *NDT and E International* 38: 654-664.
8. Altmann, J. and Mathew, J., 2001. "Multiple band-pass autoregressive demodulation for rolling-element bearing fault diagnosis". *Mechanical Systems and Signal Processing* 15: 963- 977.
9. Abbasion, S., Rafsanjani, A., Farshidianfar, A. and Irani N., 2007. "Rolling element bearings multi-fault classification based on the wavelet denoising and support vector machine". *Mechanical Systems and Signal Processing* 21: 2933- 2945.
10. Randall, R., Antoni, J. and Sawalhi, N., 2004. "Application of spectral kurtosis to bearing fault detection in rolling element bearings". *11th International Congress Sound and Vibration(ICSV11)*.
11. Young-Chul, C. and Yang-Hann, K., 2007. "Fault detection in a ball bearing system using minimum variance cepstrum". *Measurement Science and Technology* 18: 1433-1440.
12. Trendafilova, I., 2010. "An automated procedure for detection and identification of ball bearing damage using multivariate statistics and pattern recognition". *Mechanical Systems and Signal Processing* 24: 1858-1869.
13. Rauber, T. W., do Nascimento, E. M., Wandekokem, E. D. and Varejo, F. M., 2010. "Pattern Recognition based Fault Diagnosis in Industrial Processes: Review and Application". *InTech*.
14. Ericsson, S., Grip, N., Johansson, E., Persson, L.-E., Sjoberg, R. and Stromberg, J.-O., 2005. "Towards automatic detection of local bearing defects in rotating machines". *Mechanical systems and signal processing* 19: 509-535.
15. Lazzarini, B. and Volpi, S., 2013. "Classifier ensembles to improve the robustness to noise of bearing fault diagnosis". *Pattern Analysis and Applications* 16: 235-251.

16. Samanta, B., Al-Balushi, K. and Al-Araimi, S., 2003. "Artificial neural networks and support vector machines with genetic algorithm for bearing fault detection". *Engineering Applications of Artificial Intelligence* 16: 657- 665.
17. Jack, L. and Nandi, A., 2002. "Fault detection using support vector machines and artificial neural networks, augmented by genetic algorithms". *Mechanical Systems and Signal Processing* 16: 373-390.
18. Rojas, A. and Nandi, A. K., 2006. "Practical scheme for fast detection and classification of rolling-element bearing faults using support vector machines". *Mechanical Systems and Signal Processing* 20: 1523-1536.
19. Samanta, B. and Al-Balushi, K., 2003. "Artificial neural network based fault diagnostics of rolling element bearings using time-domain features". *Mechanical Systems and Signal Processing* 17: 317-328.
20. Yang, B. S., Han, T. and An, J. L., 2004. "ARTKOHONEN neural network for fault diagnosis of rotating machinery". *Mechanical Systems and Signal Processing* 18: 645-657.
21. Zhang, L., Jack, L. B. and Nandi, A. K., 2005. "Fault detection using genetic programming". *Mechanical Systems and Signal Processing* 19: 271-289.
22. Sugumaran, V. and Ramachandran, K. I., 2007. "Automatic rule learning using decision tree for fuzzy classifier in fault diagnosis of roller bearing". *Mechanical Systems and Signal Processing* 21: 2237-2247.
23. Kankar, P., Sharma, S. C. and Harsha, S., 2011. "Fault diagnosis of ball bearings using machine learning methods". *Expert Systems with Applications* 38: 1876-1886.
24. Sugumaran, V. and Ramachandran, K. I., 2011. "Effect of number of features on classification of roller bearing faults using SVM and PSVM". *Expert Systems with Applications* 38: 4088-4096.
25. Saimurugan, M., Ramachandran, K. I., Sugumaran, V. and Sakthivel, N. R., 2011. "Multi component fault diagnosis of rotational mechanical system based on decision tree and support vector machine". *Expert Systems with Applications* 38: 3819-3826.
26. Antoni, J., 2005. "Matlab code to compute signal's fast kurtogram". Accessed online on 30th June, 2014. [https://github.com/amaggi/seismokurt/blob/master/originals/matlab/Fast Kurtogram.m](https://github.com/amaggi/seismokurt/blob/master/originals/matlab/Fast%20Kurtogram.m)
27. Patil, M., Mathew, J. and RajendraKumar, P., 2008. "Bearing signature analysis as a medium for fault detection: a review". *Journal of Tribology* 130: 014001.
28. Vigya and Ghose, Tirthadip, 2016. "Artificial Intelligence and Evolutionary Computations in Engineering Systems: Chapter- Filtration of Noise in Images Using Median Filter". Springer.
29. Li, B., Chow, M.-Y., Tipsuwan, Y. and Hung J., 2000. "Neural-network-based motor rolling bearing fault diagnosis". *IEEE Transactions on industrial electronics* 47: 1060-1069.